

**Overview of the optical properties of
metals, insulators and semiconductors**

v. 3

3.5.2021

Metals

- Characteristics:

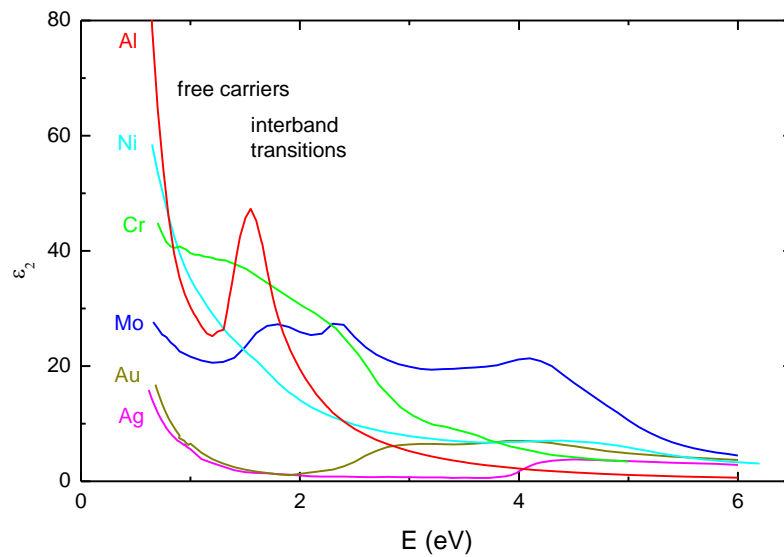
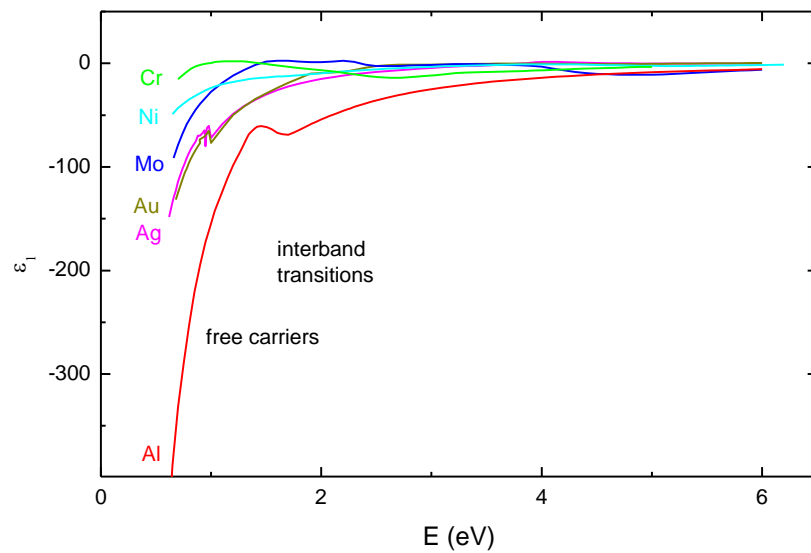
large concentration of free electrons; infrared polarizability due to the free charge carriers is typically very high, decreasing monotonically towards larger frequencies.

- The contribution of free carriers overlaps that of interband electronic transitions.

- Decreasing real part of the dielectric function with decreasing photon energy E is a characteristic feature of the free-carrier response; in the dc field ($E=0$), a finite (negative) value is reached. This behavior is linked to the diverging imaginary part of the dielectric function for $E \rightarrow 0$.

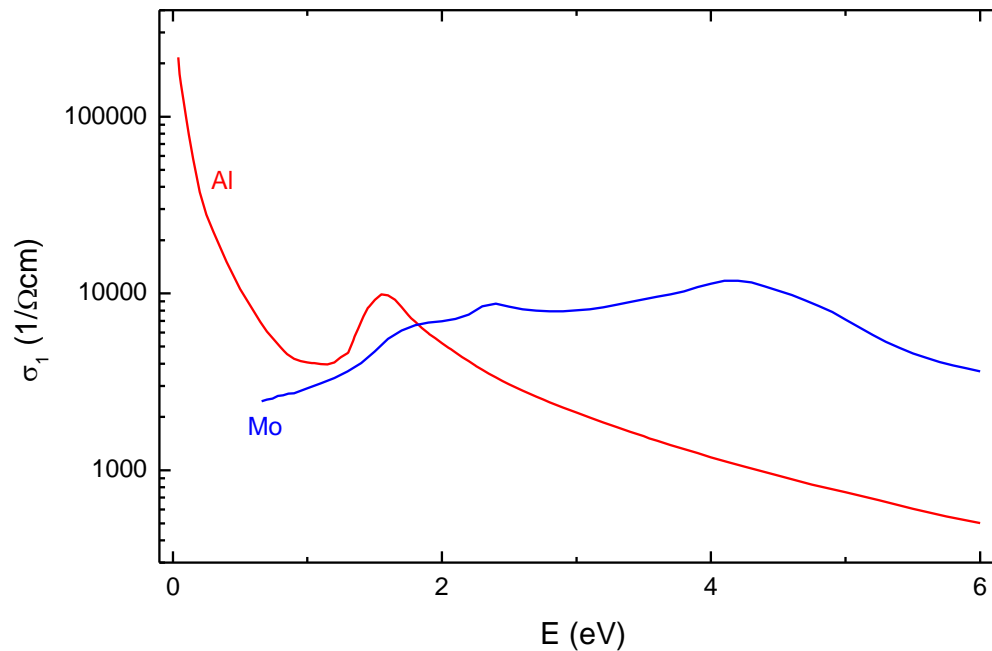
Optical conductivity remains finite; this might be the reason for using it, in particular in the infrared range.

Real and imaginary part of the complex dielectric function of several elemental metals.



Real part of the complex conductivity of Al and Mo

- Direct-current conductivity of pure Al and Mo at room temperature is 3.77×10^5 and 1.87×10^5 $1/\Omega\text{cm}$, respectively; in the infrared data of Al, the *dc* value is almost reached at the lowest photon energy. On the contrary, the conductivity of Mo has to increase below the lowest photon energy in the shown spectrum.
- The monotonic contribution of free electrons overlaps with that of the interband transitions. In the spectra of Al, the latter is dominated by a relatively sharp band located at about 1.6 eV; the interband transitions in Mo form a more complex contribution, including evidently rather low photon energies.

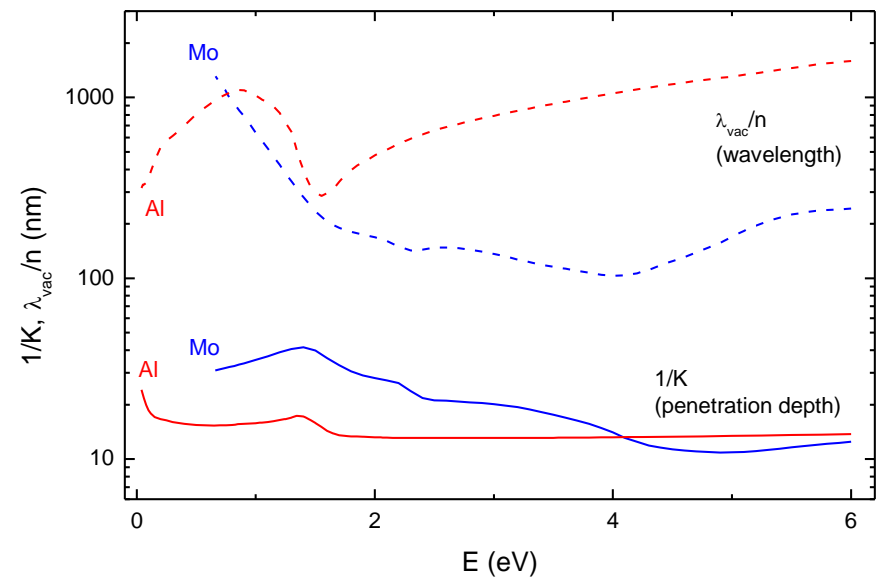
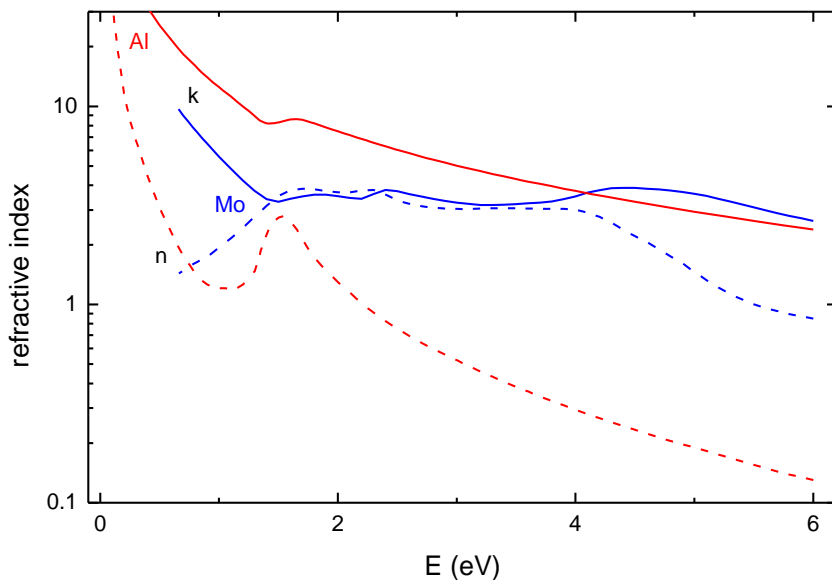


Complex refractive index of Al and Mo

Optical spectra of Aluminum display a typical “metallic” behavior. The complex refractive index, $n+ik$, has its real part (n) noticeably smaller than the real one (k). This is due to the prevailing influence of free electrons` in this sense, the response of Molybdenum is “less metallic”. In “ideal metal” at positive frequencies, smaller than the plasma frequency, the dielectric function is real and negative; its square root is therefore pure imaginary.

Complex refractive index is instrumental in dealing with the propagation of light waves in homogeneous material (via wavelength and decay of the amplitude) and in investigating the phenomena at interfaces (using, e.g., Fresnel formulae for the amplitude reflectance and transmittance).

The penetration depth of light ($1/K$) in the optical range is typically rather small, of the order of tens of nanometers. This is the reason for the opacity of metallic films even of rather small thicknesses. Note also the large values of the wavelength in Al in the ultraviolet.



Au, problems related to sample quality and spectral measurements

Gold: relatively stable surfaces of (poly)crystals, evaporation and sputtering

Aspnes 1980, ellipsometric results and previous measurements

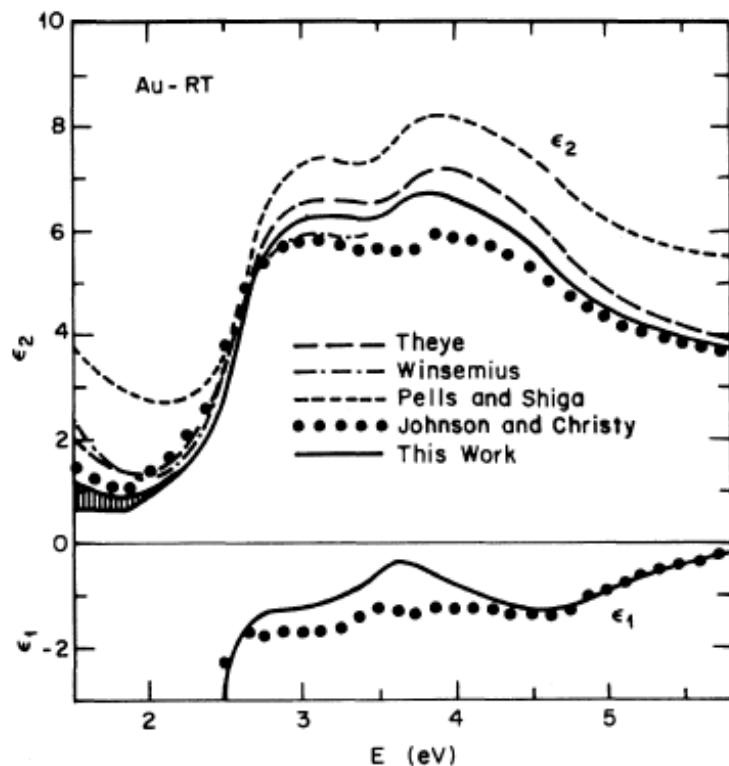


FIG. 1. Representative dielectric-function data for Au: Thèye (Ref. 14), thin film, UHV evaporated and annealed; Winsemius (Ref. 25), bulk polycrystal, UHV annealed; Pells and Shiga (Ref. 21), as Winsemius; Johnson and Christy (Ref. 15), unannealed thin film; this work, electron-beam evaporated thin film.

Au, problems related to sample quality and spectral measurements

Aspnes 1980, ellipsometric measurements, films evaporated at low (LN) and room temperatures of the substrate (for low temperatures – worse crystallinity of the films, stronger scattering of free electrons).

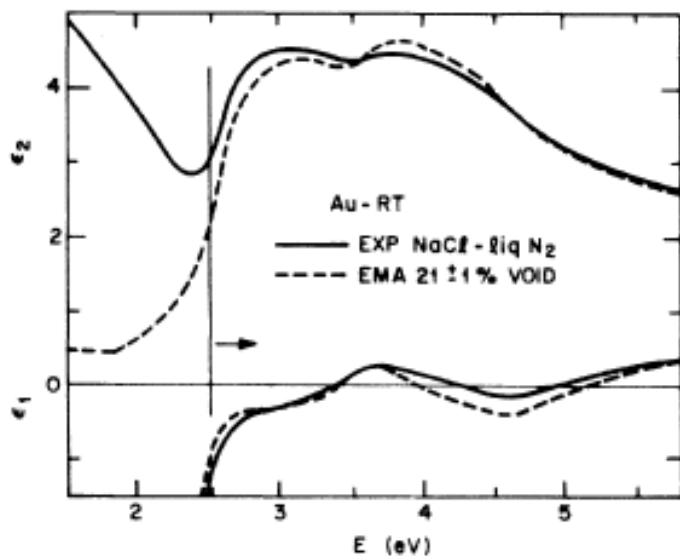


FIG. 7. Comparison of liquid-N₂ thin-film sample spectra from Fig. 2 with a one-parameter EMA calculation assuming 21% voids.

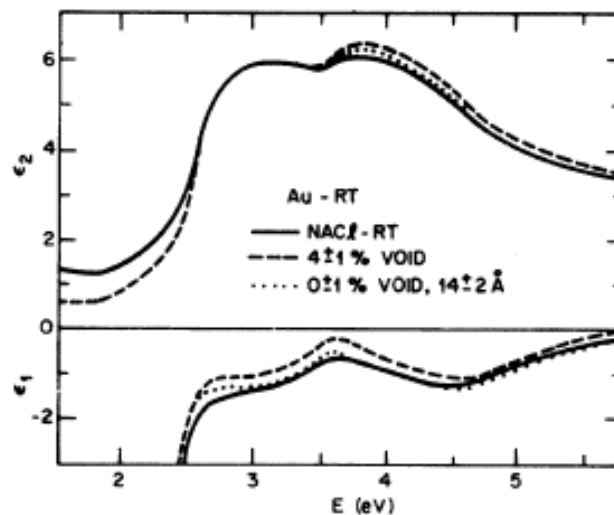
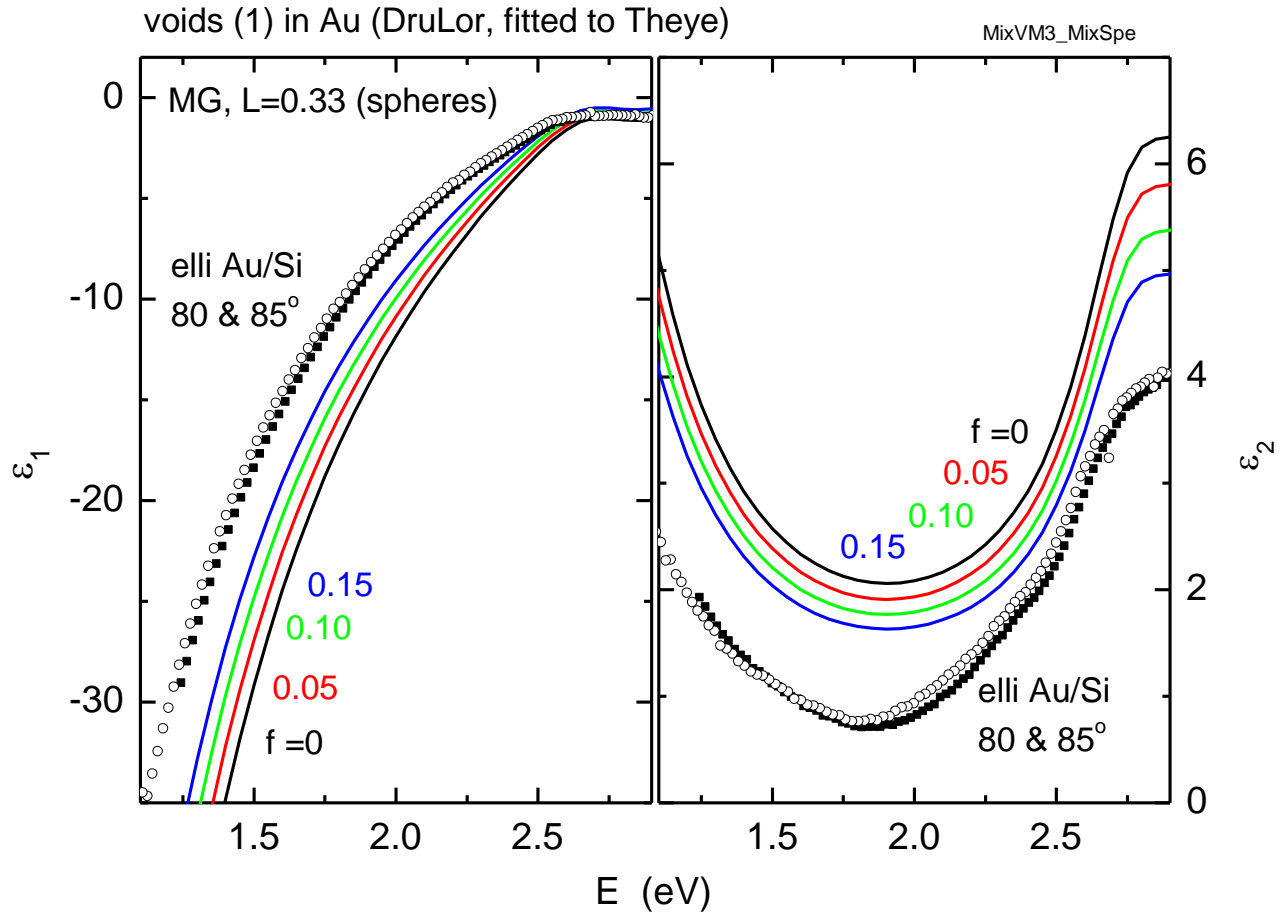


FIG. 8. Same as Fig. 7, but for the RT thin-film sample of Fig. 2. Also shown are the results of a two-parameter calculation assuming voids and an overlayer film.

Au, problems related to sample quality and spectral measurements

Au / Si, evaporated at DCMP Brno (2000); ellipsometric data in accord with the assumption of a porous overlayer (~10 nm thick)



Au, problems related to sample quality and spectral measurements

high-quality massive polycrystals of Au, Ag and Cu: Otter 1961; ellipsometric data on curved samples with no surface treatment

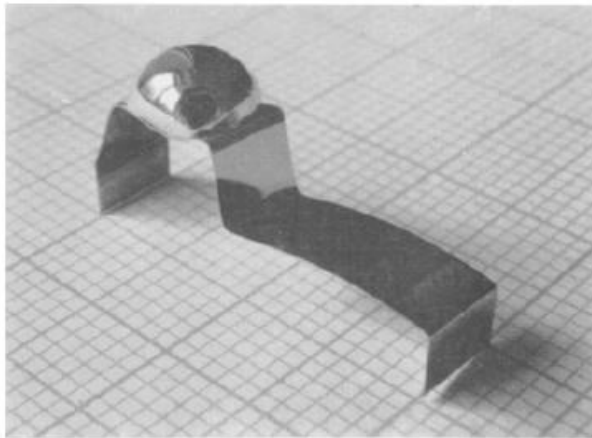


Fig. 1. Kupferprobe auf dem Wolframband

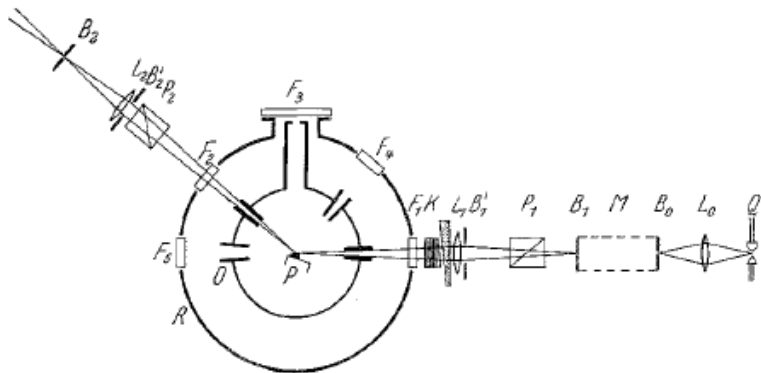


Fig. 2. Vertikaler Schnitt durch die Präparations- und Meßanordnung (schematisch)

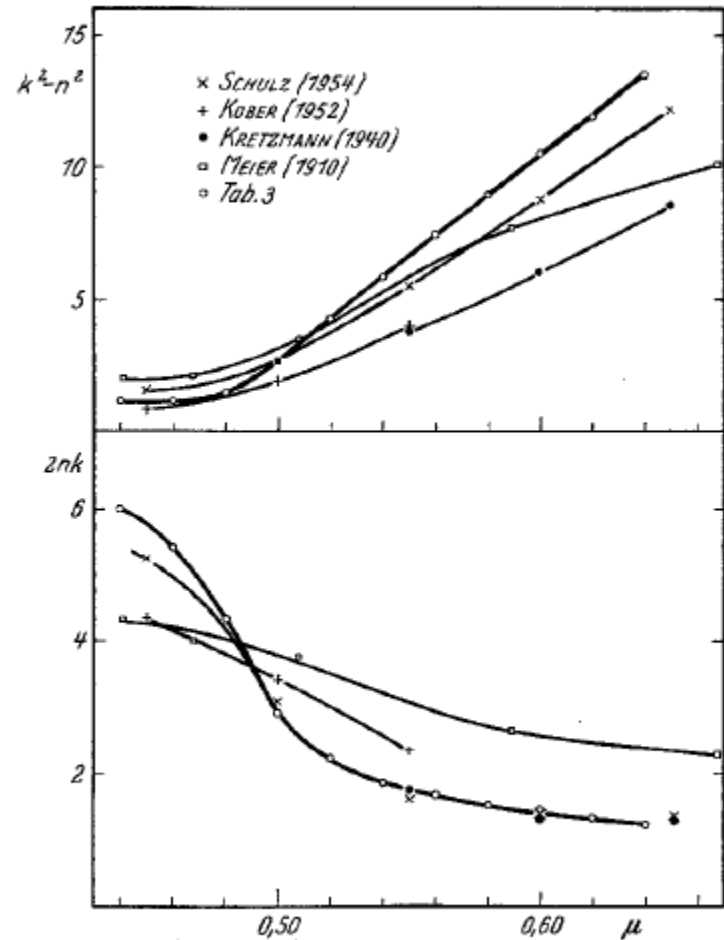
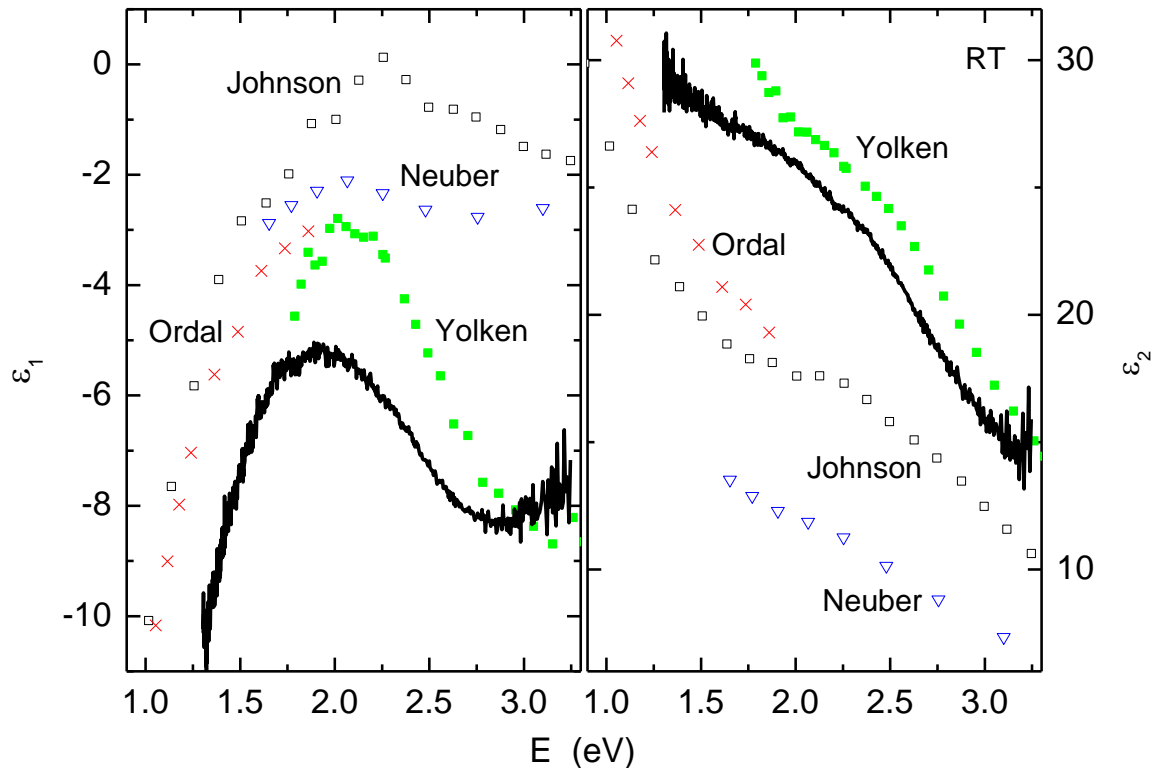


Fig. 5. Optische Konstanten von Au. Mittelwerte von drei Einkristallproben. Vergleich mit früheren Messungen. 20° C

Fe: free electrons and interband transitions



Large differences between dielectric functions; solid lines – ellipsometric data measured at DCMP (2007); difficult preparation of good samples.

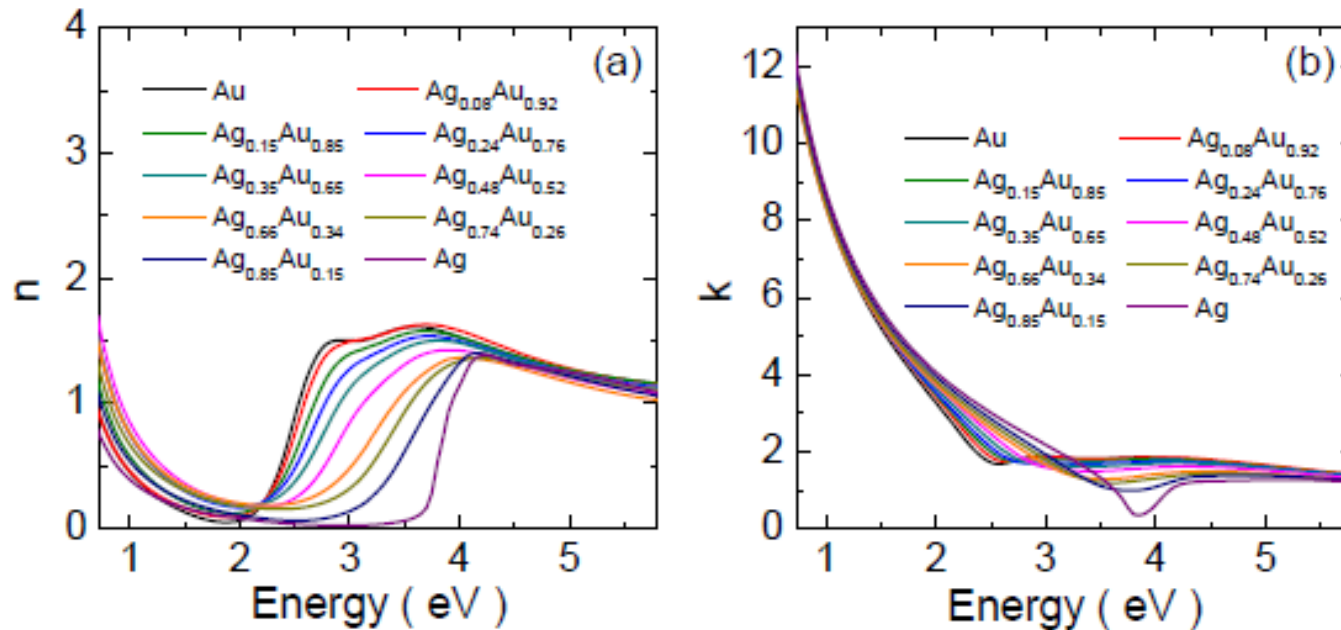
Drude-like response of free electrons is negligible in the absorptive part (ϵ_2), however, very well resolved in the real part (ϵ_1).

Example of an alloy: $\text{Ag}_x \text{Au}_{1-x}$

Alloys usually display properties typical of modifications of their components.

Ag + Au: Peña-Rodríguez (2014), evaporated films (170 – 330 nm on Si, co-deposition by electron-beam evaporation of Ag and Au, the thickness and composition obtained from RBS), ellipsometric spectra.

Differences seen in the free electron response (eps. in NIR), and also in the onset of the strong interband absorption (almost 1.5 eV higher in Ag than in Au).



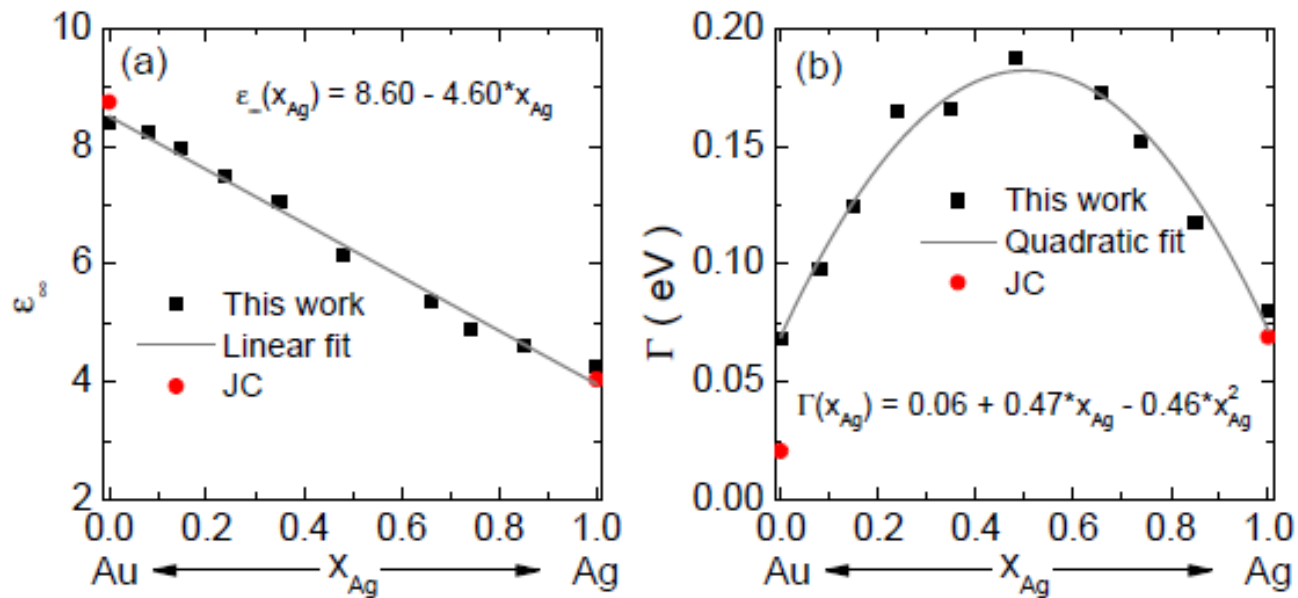
Example of an alloy: $\text{Ag}_x \text{Au}_{1-x}$

Ag + Au: Peña-Rodríguez (2014)

Parametrization of the free electron response – Drude model (JC=“Johnson-Christy” for both endpoints).

Plasma energy almost independent of the composition ($E_p \approx 9$ eV).

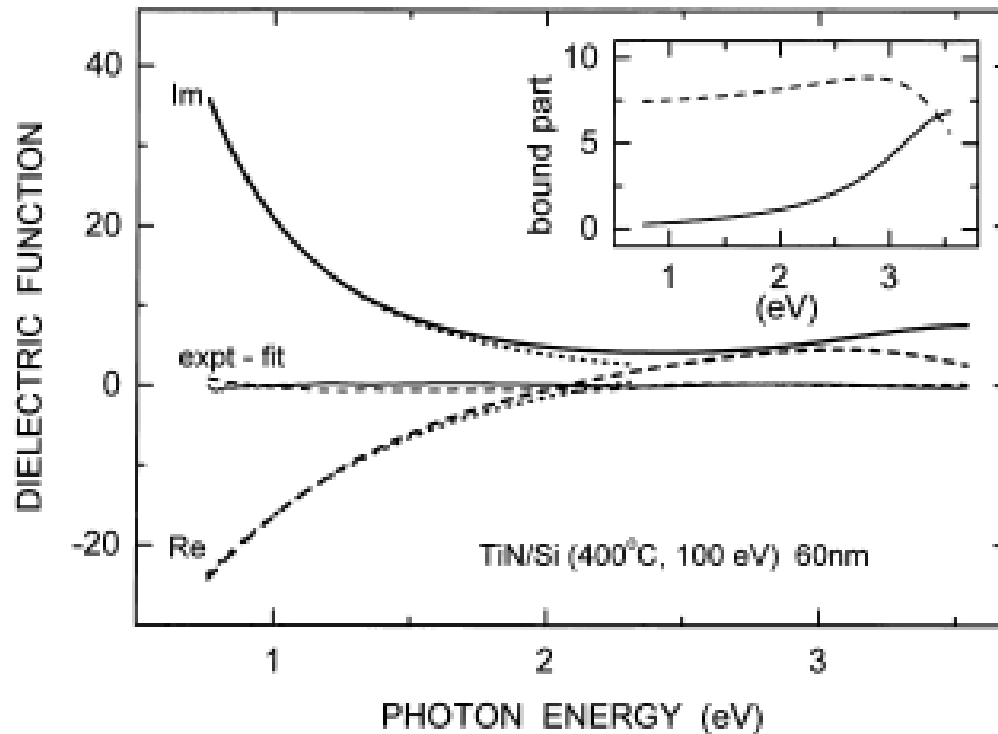
Typical dependence, $\sim x(1-x)$, of the broadening parameter is due primarily to the electron scattering on the potential of randomly distributed atoms in the alloy.



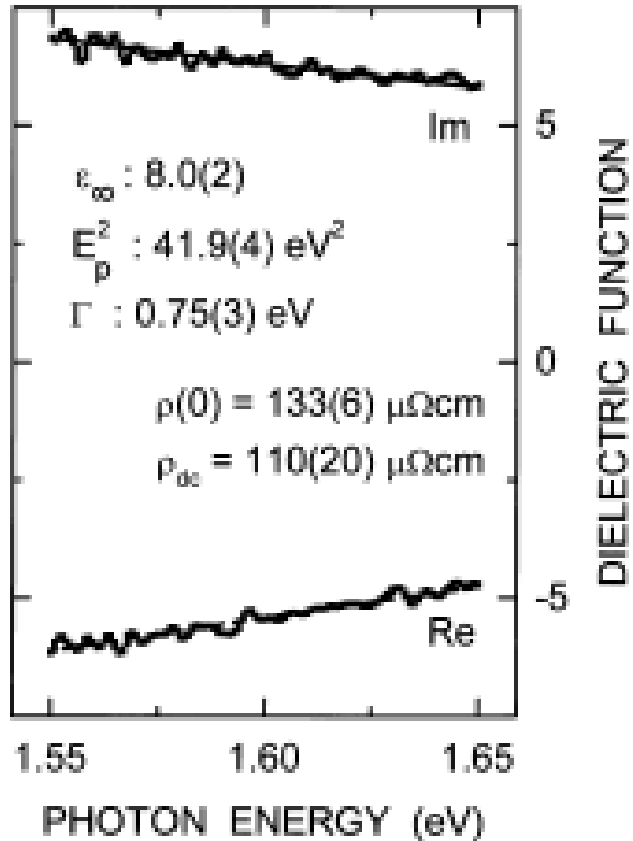
“Metallic behavior” of TiN

A number of compounds contains large density of free charge carriers, leading to the optical response similar to elementary metals and their alloys. TiN is a very hard compound, with the color similar to that of gold.

In IR, the dominant polarizability is that of free electrons, in UV that of the interband transitions; the sum of Drude contribution and a broad Lorentzian band (at ~ 3.6 eV) fits very well the measured ellipsometric spectra.



Free electrons in v TiN

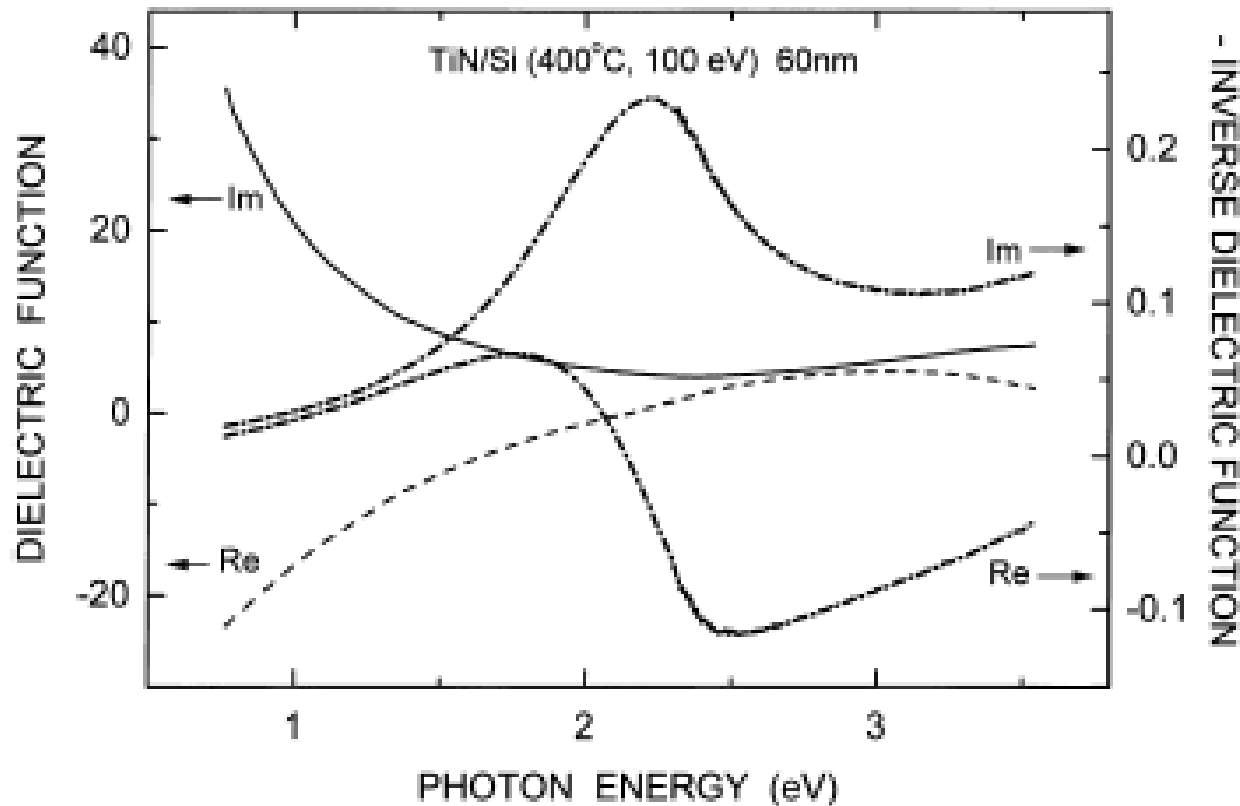


Parametrization using the Drude model in a narrow spectral range;

fairly good agreement of the dc resistivity with the extrapolation to zero frequency (in Ωcm with both energies in eV):

$$\rho(0) = 0.007435 \frac{\Gamma}{E_p^2}$$

The overlap of free-electron response with interband transitions in TiN:
plasmon resonance in the visible range:

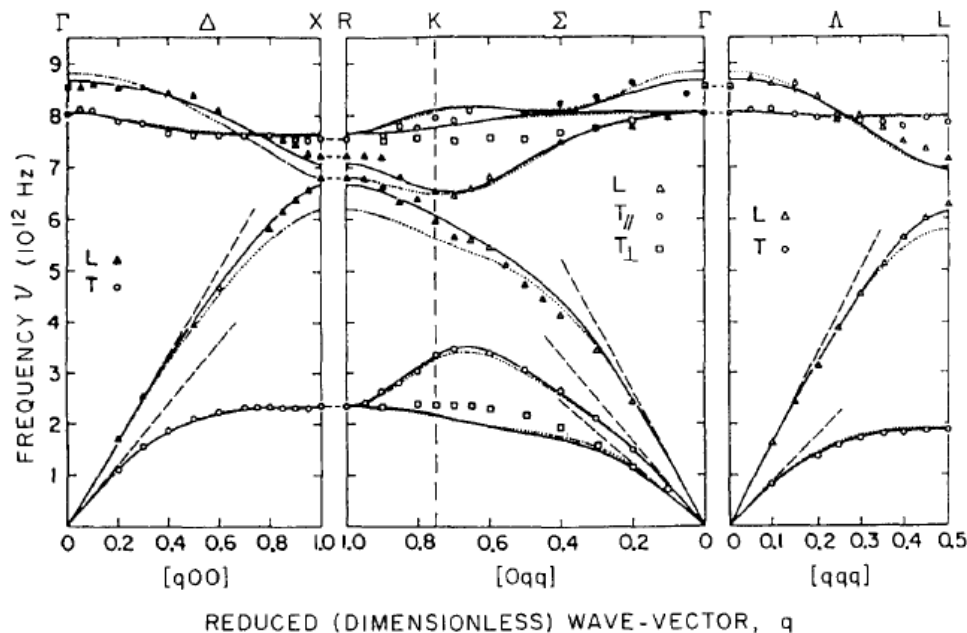


The negative inverse of the dielectric function displays the band of increased absorption of longitudinal waves at 2.2 eV, in a good agreement with EELS data.

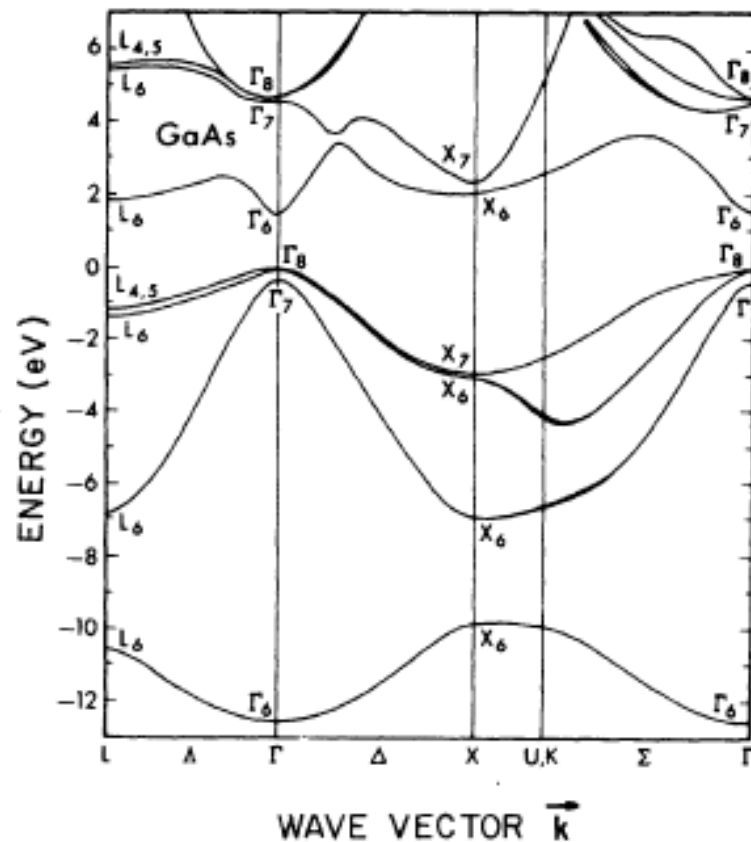
Crystalline semiconductors and insulators

translational symmetry \rightarrow dispersion of energies (k -dependence) of single-particle states
 the quasiparticles are

bosons



fermions



An instructive case study - doped (n-type) crystalline GaAs

low frequencies (FIR-MIR):

- free-electron plasma, small effective mass, large mobility
- polar lattice vibrations, TO ~ 8 THz (34 meV), LO ~ 8.5 THz

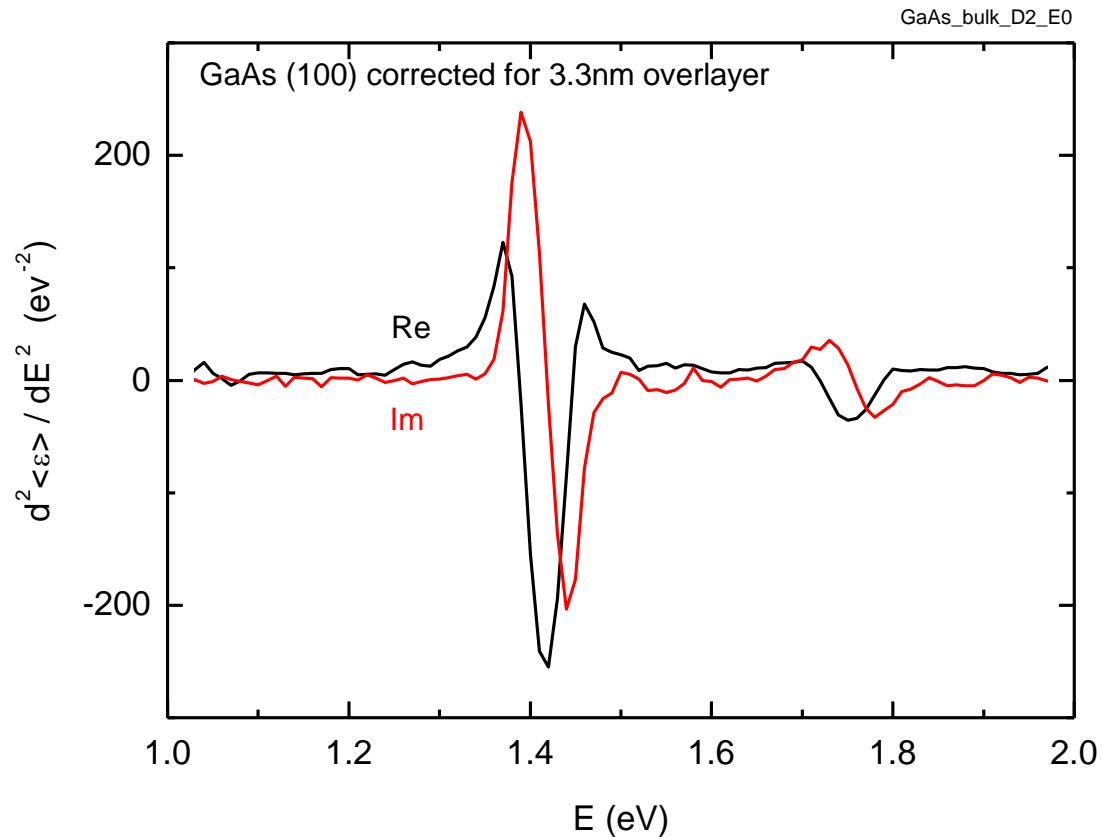
larger frequencies (NIR, VIS, UV):

- onset of interband transitions (1.42 eV at RT)
- strong variations of the joint density of states above gap, in particular in UV
- strong influence of final-state (excitonic) interaction

Spectra at the onset of absorption near the gap energy, undoped GaAs
(„epiready“ sample, several years in the laboratory atmosphere; ellipsometric measurements)
a strong influence of the excitonic interaction on the $3DM_0$ direct gap

$$E_g = 1.42 \text{ eV @RT}$$

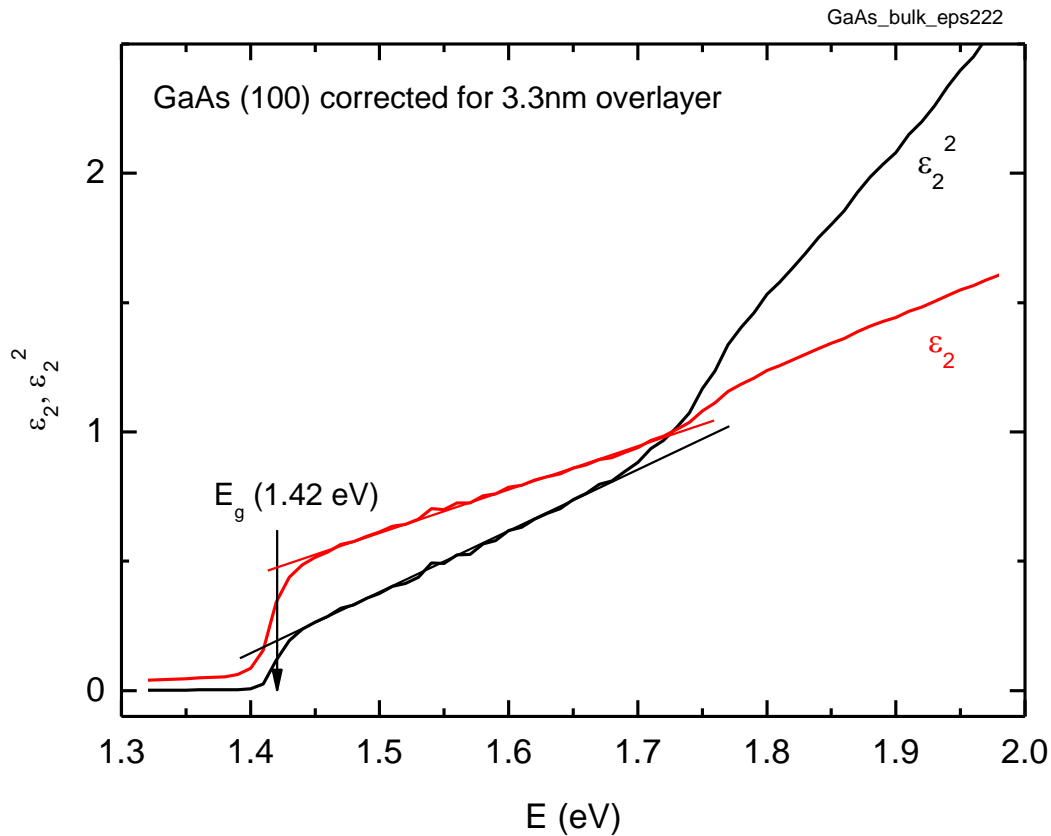
second derivative of the dielectric function (corrected for the presence of a non-absorbing overlayer)



Undoped GaAs – ellipsometric data

$E_g = 1.42 \text{ eV @RT}$

the dangerous extrapolations of the spectral dependences



Several insulators and semiconductors, crystalline and amorphous ("glassy") materials

LiF

α -SiO₂

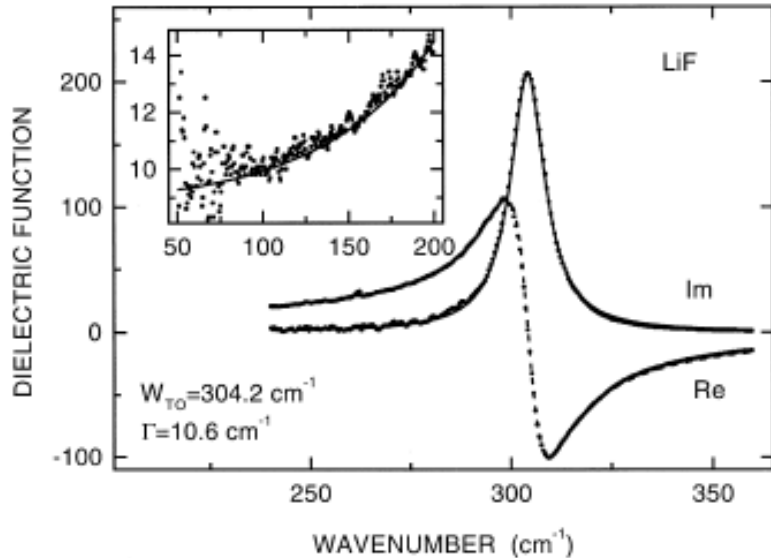
intrinsic crystalline Si

 multiphonon absorption, transparent range
 interband transitions

Si:P, metal-insulator transition

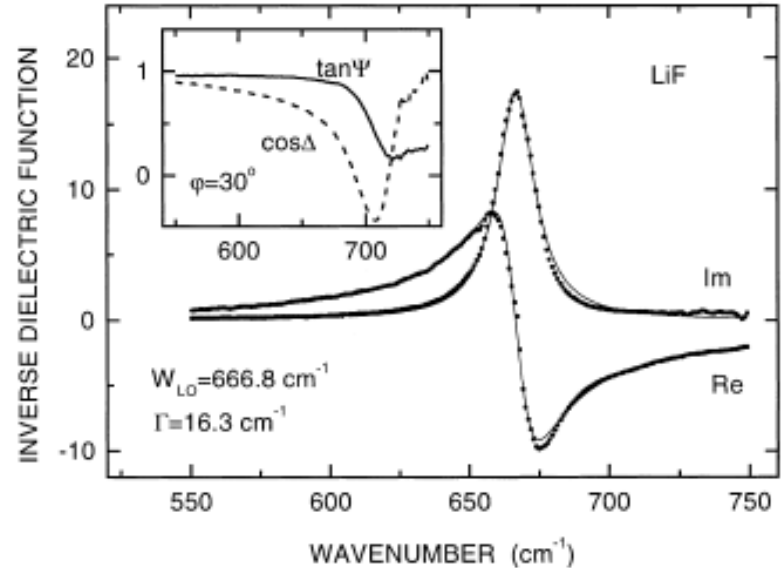
Lattice vibrations in polar crystals: LiF

FIR (TO) + MIR (LO) ellipsometry, JH, Thin Solid Films **313-314** (1998), 687-691



Dielectric function:
(resonance of the IR wave with the TO phonon)

Lorentzian profile of the band
extrapolation of the real part gives the static permittivity
noticeable broadening at RT



Negative inverse of the dielectric function:
(“LO-resonance“)

nearly Lorentzian lineshape
the width influenced by the presence of multiple-phonon absorption

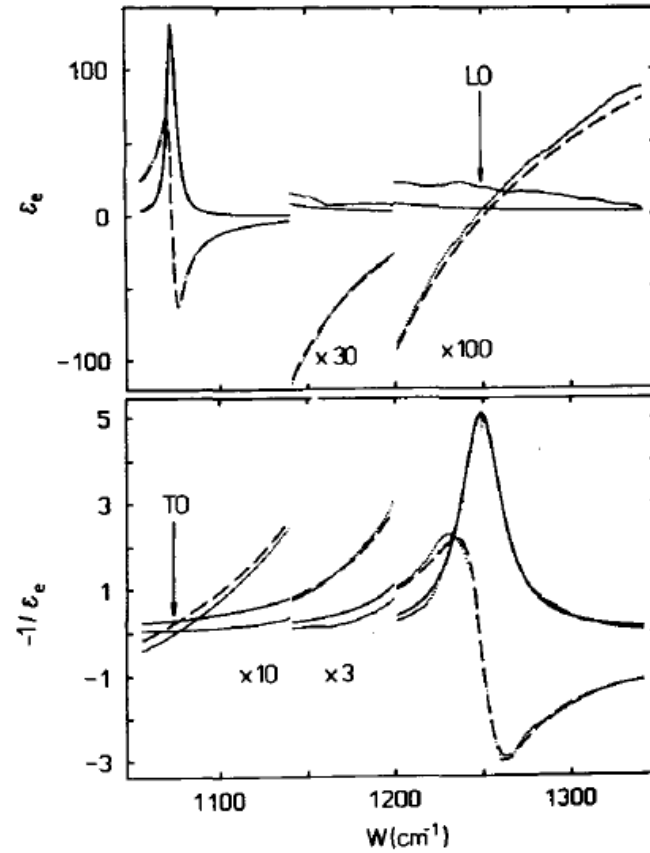
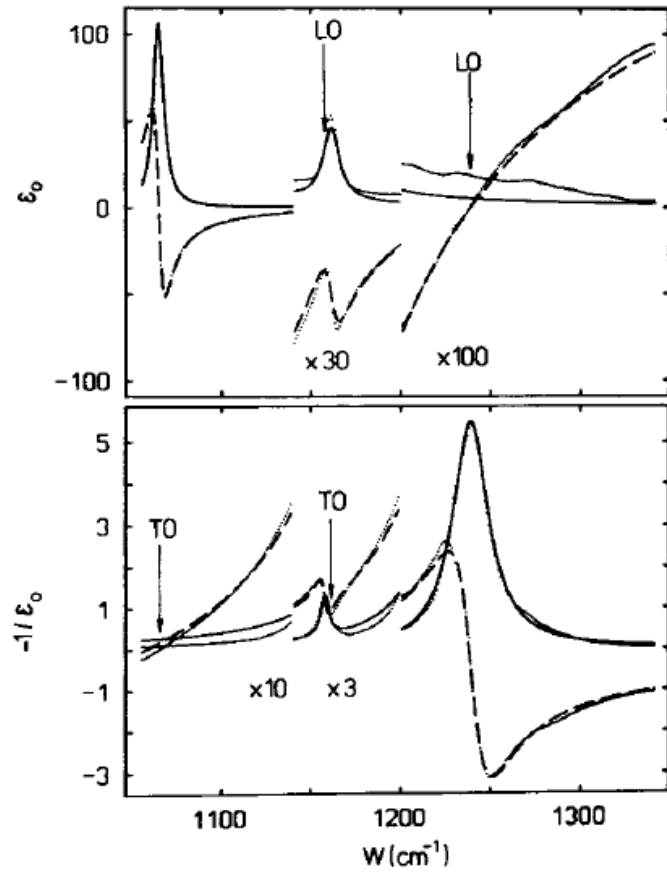
Lattice vibrations of a more complex polar crystal: α -SiO₂

Anisotropic (uniaxial) crystal:

several TO and LO modes identifiable in ϵ and $-1/\epsilon$ for ordinary and extraordinary direction;
most of the bands fairly narrow (small broadening parameters Γ)

l	F_l (10^5 cm^{-2})	W_l (cm^{-1})	Γ_l (cm^{-1})
Ordinary ray (E-modes)			
TO ₁	1.78 ± 0.01	449.5 ± 0.2	4.0 ± 0.1
LO ₁	0.144 ± 0.001	508.1 ± 0.1	3.8 ± 0.1
TO ₂	0.12 ± 0.02	695.0 ± 0.2	8.2 ± 2.0
LO ₂	0.0074 ± 0.0002	697.5 ± 1.0	5.9 ± 1.0
TO ₃	0.79 ± 0.02	795.2 ± 0.2	7.9 ± 0.5
LO ₃	0.056 ± 0.002	808.8 ± 0.3	7.1 ± 0.3
TO ₄	7.95 ± 0.03	1065.0 ± 0.2	7.0 ± 0.2
LO ₄	1.64 ± 0.01	1238.7 ± 0.3	24.1 ± 0.5
TO ₅	0.18 ± 0.04	1161 ± 1	12 ± 4
LO ₅	0.018 ± 0.002	1157.5 ± 1.0	4.8 ± 1.0
Extraordinary ray (A ₂ modes)			
TO ₁	1.88 ± 0.02	494.5 ± 0.2	5.6 ± 0.1
LO ₁	0.157 ± 0.002	552.2 ± 0.1	5.0 ± 0.2
TO ₂	0.74 ± 0.02	775.7 ± 0.2	6.5 ± 0.3
LO ₂	0.063 ± 0.002	789.2 ± 0.3	6.9 ± 0.3
TO ₃	8.68 ± 0.03	1073.4 ± 0.2	6.1 ± 0.1
LO ₃	1.76 ± 0.01	1248.5 ± 0.3	27.6 ± 0.5

Interlacing of TO and LO modes in α -SiO₂



Ellipsometric data and best-fit Lorentzians, ordinary and extraordinary direction

Transparent range between lattice vibrations (IR) and electronic absorption (UV) in α -SiO₂

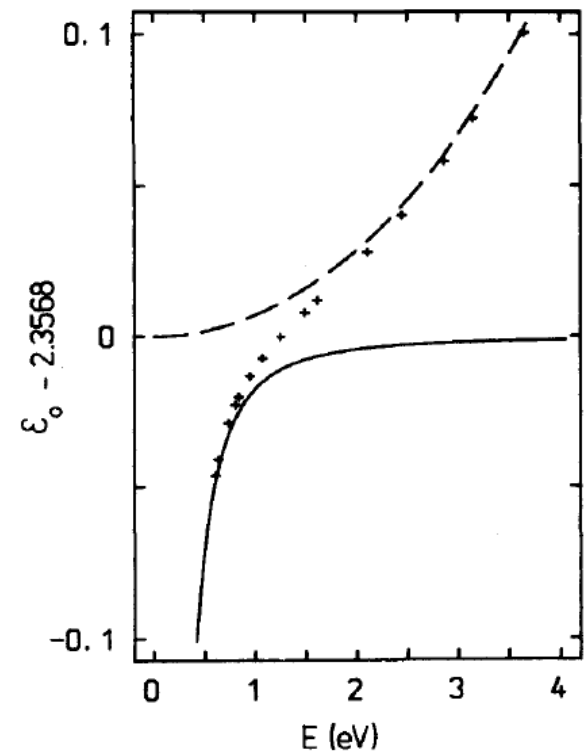
Dielectric function is real (conductivity is imaginary); the dispersion of optical functions can be very precisely ($\sim 10^{-5}$) approximated by the expansion

$$\epsilon(E) \approx \sum_j a_{2j} E^{2j}$$

using 2 “phonon” terms ($j=-1,-2$) and 4 “electron” terms ($j=0,\dots,3$)

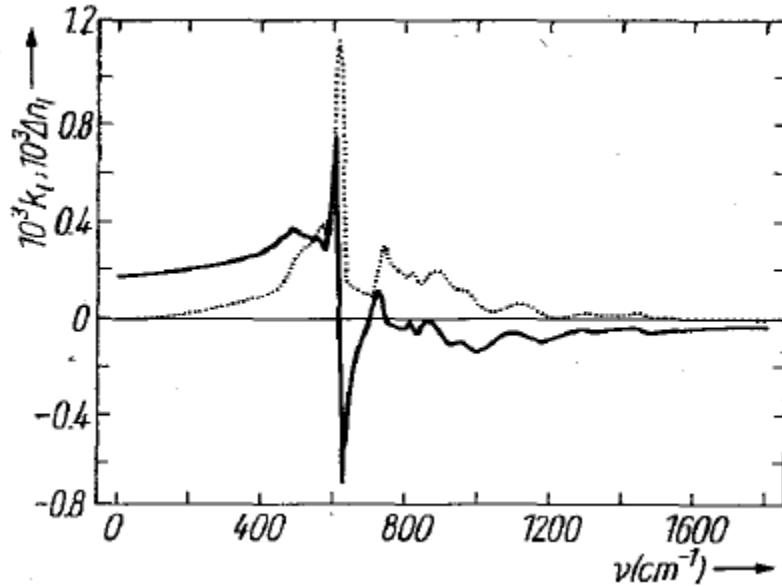
	a_{-4} (10^{-4} eV^4)	a_{-2} (10^{-2} eV^2)
Ordinary	-1.8 ± 0.3	-1.73 ± 0.01
Extraordinary	-1.4 ± 0.4	-1.83 ± 0.01

a_0	a_2 (10^{-3} eV^{-2})	a_4 (10^{-5} eV^{-4})	a_6 (10^{-7} eV^{-6})
2.3568 ± 0.0001	6.95 ± 0.02	4.6 ± 0.1	4.3 ± 0.2
2.3841 ± 0.0001	7.19 ± 0.02	5.0 ± 0.1	4.5 ± 0.2

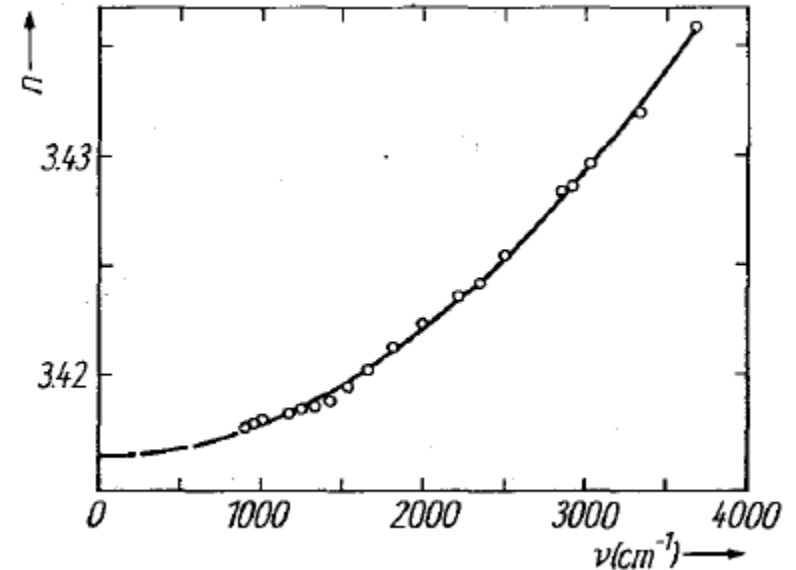


Multiphonon response of homopolar materials: intrinsic Si

MIR, transmission and reflectivity + KK analysis, JH et al., phys. stat. sol. (a) **92** (1985) 249-255



Very small absorption (slabs ~1mm thick provide easily measurable transmittance even at the maximum at 605 cm⁻¹;
spectral changes of the real part of refractive index are smaller than 0.001.



Low-frequency (MIR) part of the transparent range is described by the following parametrization of refractive index (the dispersion is due to the interband transition above gap wavenumber, ~ 9000 cm⁻¹):

$$n_1(\nu) = 3.41626 + 1.443 \times 10^{-9} \nu^2$$

Ellipsometric spectra of Si (rotating analyzer)

Aspnes (Studna, McIntyre), 1983 (c-Si)

Aspnes, Studna, Kinsbron, 1984 (a-Si)

problems in the range of small absorption above the (indirect) gap

c-Si

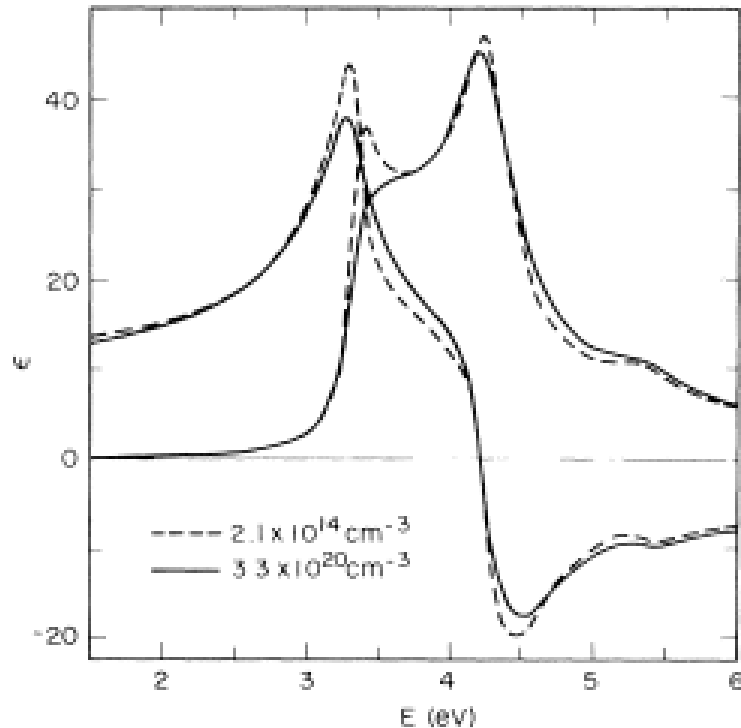


FIG. 1. Dielectric response ϵ' of a P-doped large-grain polysilicon film with $n = 3.3 \times 10^{20} \text{ cm}^{-3}$. Pseudodielectric function (ϵ') from Ref. 15 of a lightly doped ($n = 2.1 \times 10^{14} \text{ cm}^{-3}$) silicon crystal is also shown for comparison.

a-Si

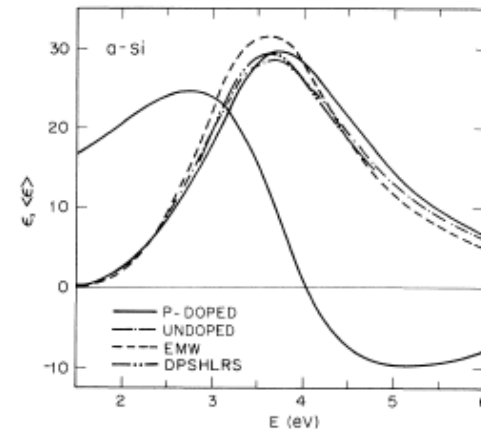


FIG. 12. Dielectric function spectra of a-Si films obtained from different sources. Solid curve: *in situ* P-doped LPCVD film, this work. Dot-dashed curve: undoped LPCVD film, from Ref. 23. Dashed curve: glow-discharge film, from Ref. 44. Double-dotted-dashed curve: multipole-plasma film, from Ref. 24.

Optical spectra of silicon in MIR-UV utilizing SOI structures and homoepitaxial samples

JOURNAL OF APPLIED PHYSICS **118**, 195706 (2015)



Optical functions of silicon from reflectance and ellipsometry on silicon-on-insulator and homoepitaxial samples

J. Humlíček^{1,a)} and J. Šik²

¹*CEITEC, Masaryk University, Kamenice 753/5, 62500 Brno, Czech Republic*

²*ON Semiconductor, 1. máje 2230, 75661 Rožnov p. Radhoštěm, Czech Republic*

(Received 8 October 2015; accepted 5 November 2015; published online 20 November 2015)

The optical properties of silicon have been determined from 0.2 to 6.5 eV at room temperature, using reflectance spectra of silicon-on-insulator (SOI) and ellipsometric spectra of homoepitaxial samples. Optimized Fabry-Perot-type SOI resonators exhibit high finesse even in near ultraviolet. Very high precision values of the real part of the refractive index are obtained in infrared up to a photon energy of 1.3 eV. The spectra of the extinction coefficient, based on observations of light attenuation, extend to 3.2 eV due to measurements on SOI layers as thin as 87 nm. These results allowed us to correct spectroellipsometric data on homoepitaxial samples for the presence of reduced and stabilized surface layers. © 2015 Author(s). All article content, except where otherwise noted, is licensed under a Creative Commons Attribution 3.0 Unported License.

[<http://dx.doi.org/10.1063/1.4936126>]

Optical spectra of silicon in MIR-UV utilizing SOI structures and homoepitaxial samples

JH et al., JAP **118** (2015) 195706

normal-incidence reflectivity in MIR+NIR (Fourier spectrometer IFS66) , NIR-VIS-UV (fiber spectrometer Avantes 2048)

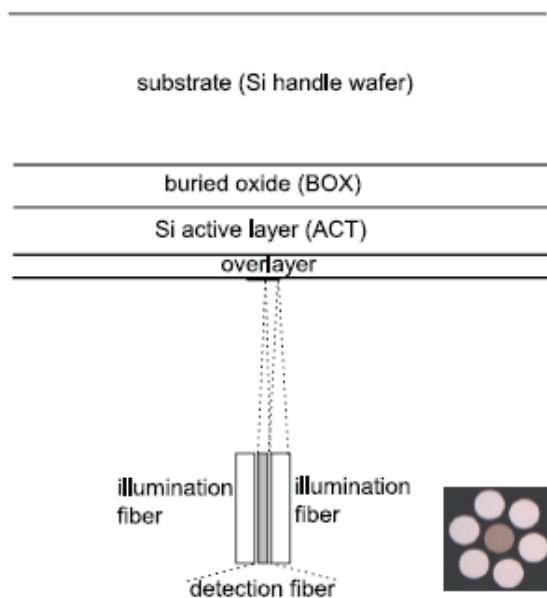


FIG. 1. Schematic representation of the SOI layered structure and the fiber reflectance probe (not to scale). Dotted lines: two limiting reflected rays; thick segment: measured spot at the sample surface. Bottom right: optical image of the termination of a reflectance probe with 6 illumination fibers surrounding the central detection fiber, each of 400 μm diameter.

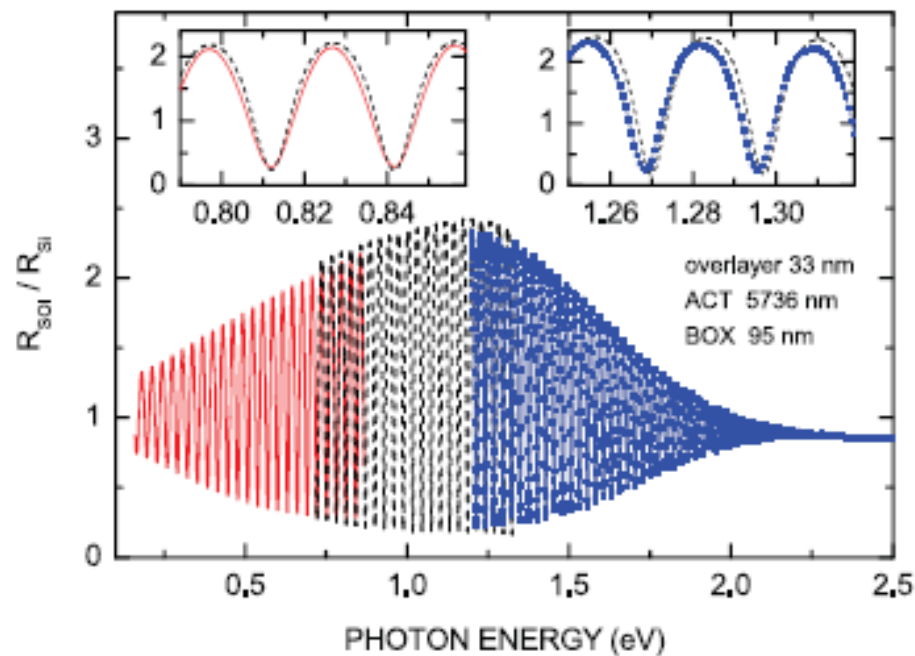
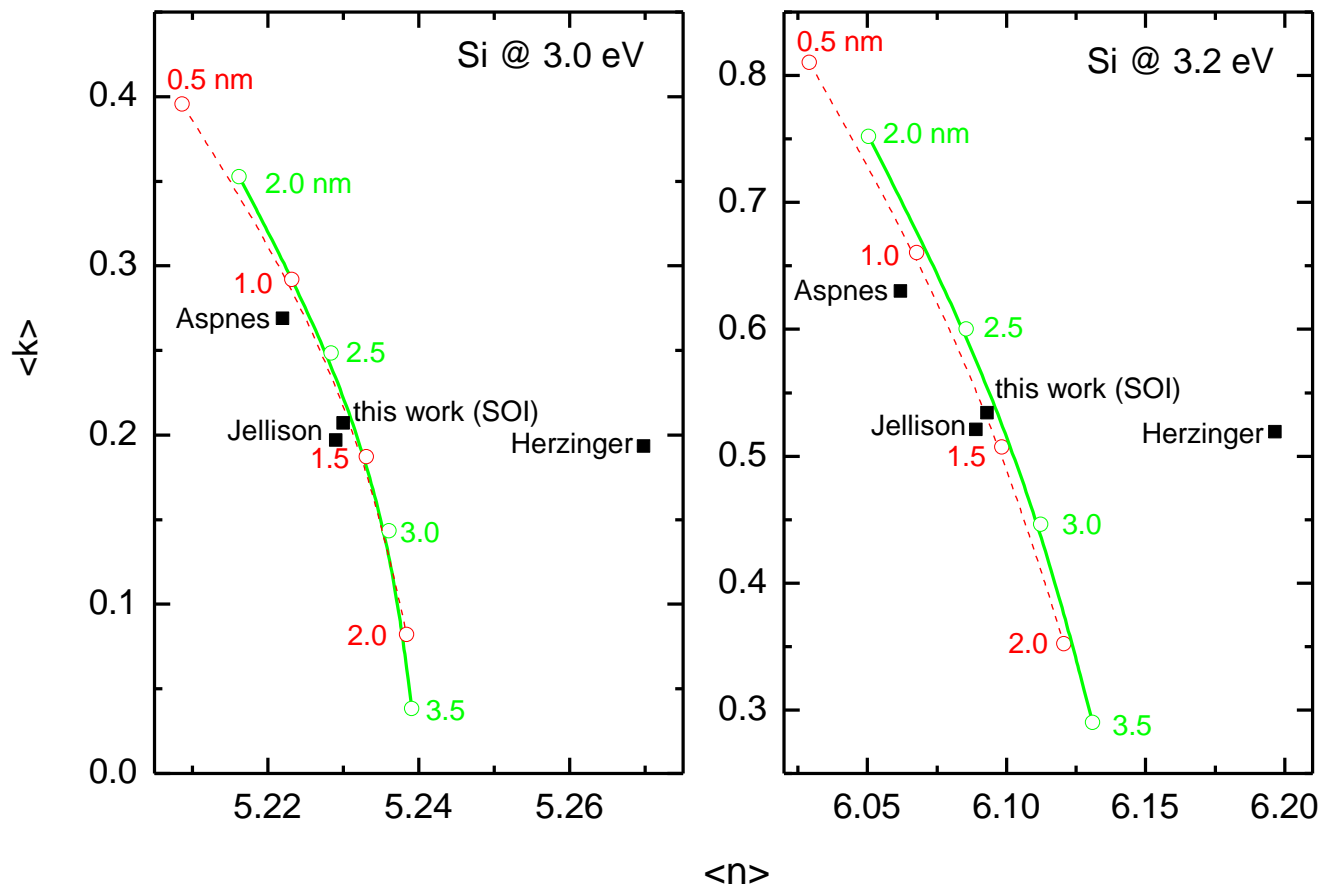


FIG. 2. Relative reflectance of the 5736 nm SOI sample, measured in MIR (red solid line) and NIR (black dashed line) at an angle of incidence of 10° , and in NIR-VIS (blue symbols) at 0.5° . Insets: a few interference fringes in the overlapping regions.

Optical spectra of silicon in MIR-UV utilizing SOI structures and homoepitaxial samples

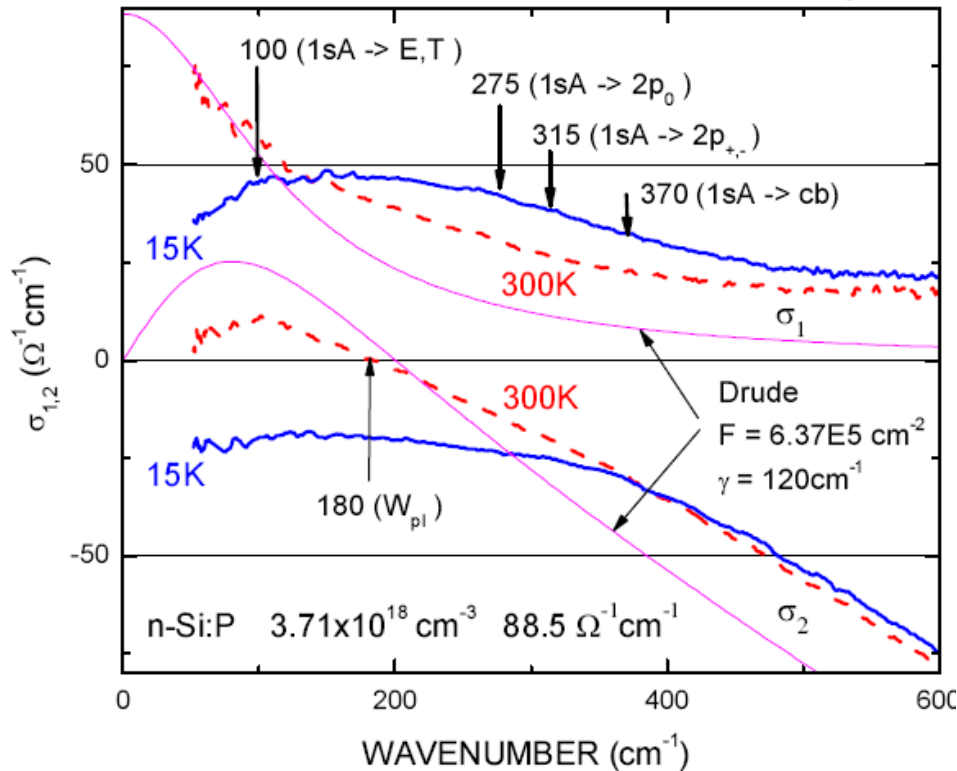
JH et al., JAP **118** (2015) 195706

Elipsometry (rotating compensator) in NIR-VIS-UV, sensitivity to surface overlayers;
utilizing the data obtained from the reflectance (at 3.0 and 3.2 eV)



Donor states and free carriers in n-type semiconductors: Si:P

FIR ellipsometry, JH et al., AIP Conf. Proc. **893** (2007) 33



Complex conductivity
(doping very close to the Metal-Insulator transition)

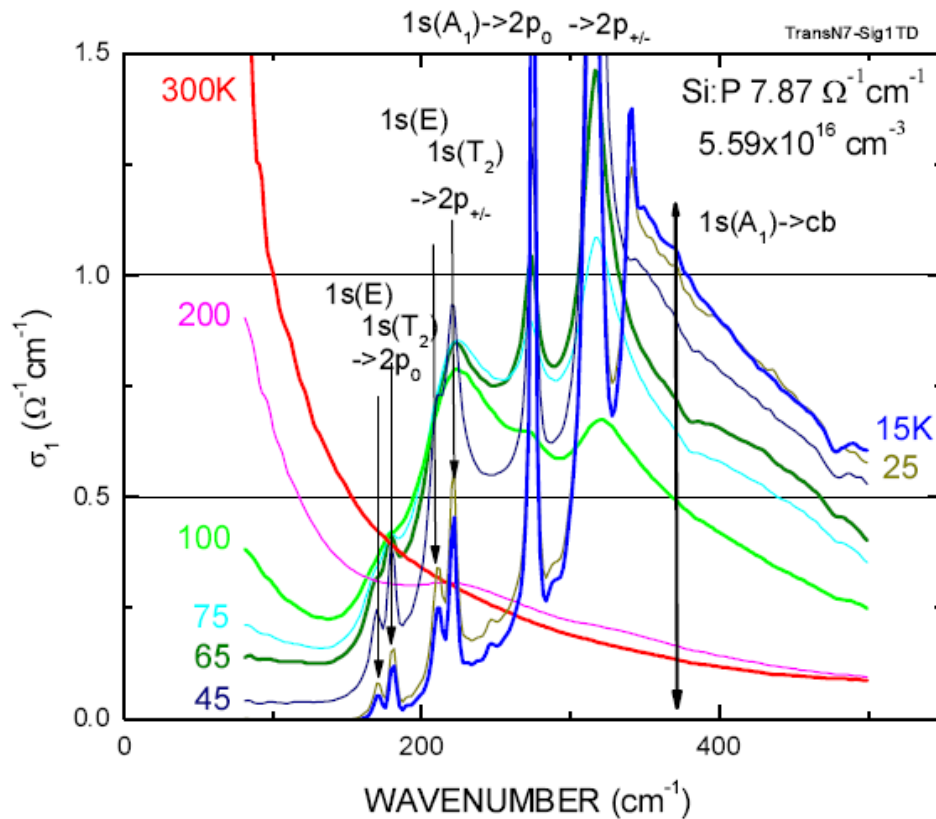
differs from the Drude lineshape even at RT

complex frequency and temperature dependences

residues from the absorption lines of diluted donors (?)

Donor states and free carriers in n-type semiconductors: Si:P

FIR transmission, JH et al., unpubl.



Free electrons freeze out with decreasing temperature

the localized electron states are responsible for the absorption lines and the donor - conduction band continuum

Amorphous insulators („glasses“)

Short range order (SRO) preserved, long range order (LRO) missing

→

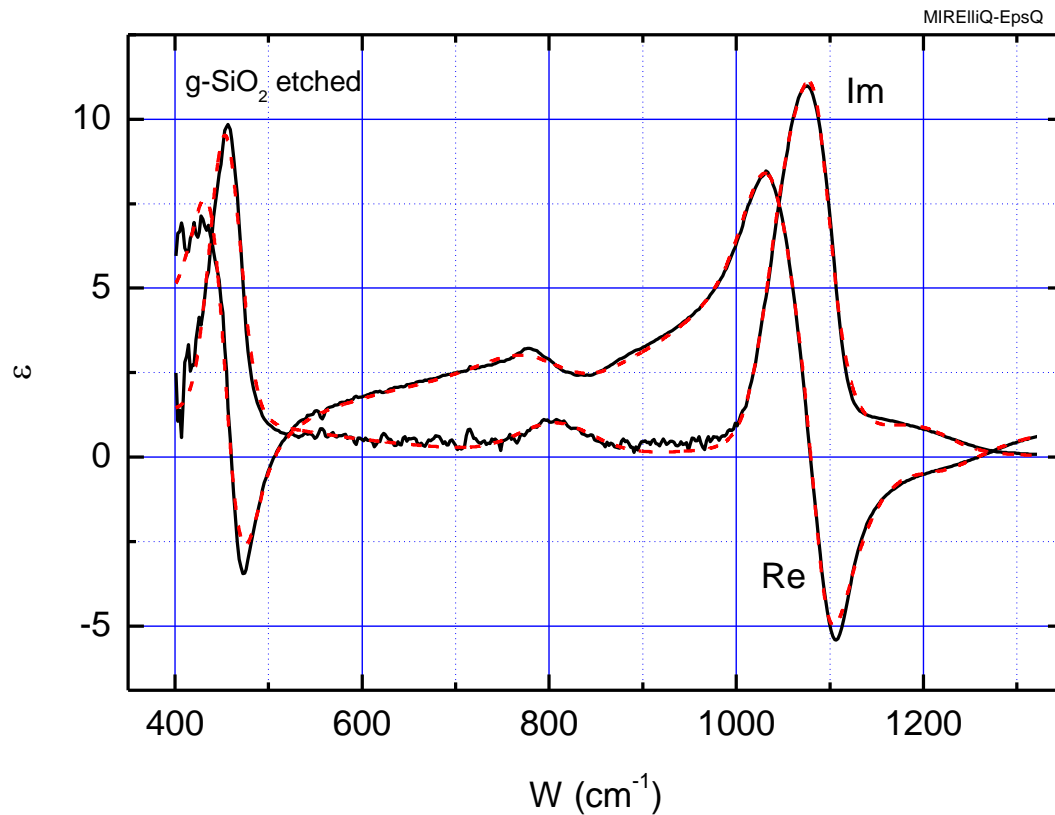
sharp structures in vibrational and electronic spectra are smeared out,

transparent range between low- and high-frequency absorption remains,
very low attenuation of the light waves is attainable (optical fibers).

Vibrations in amorphous polar materials: glassy SiO₂

elipsometry in, JH, unpublished

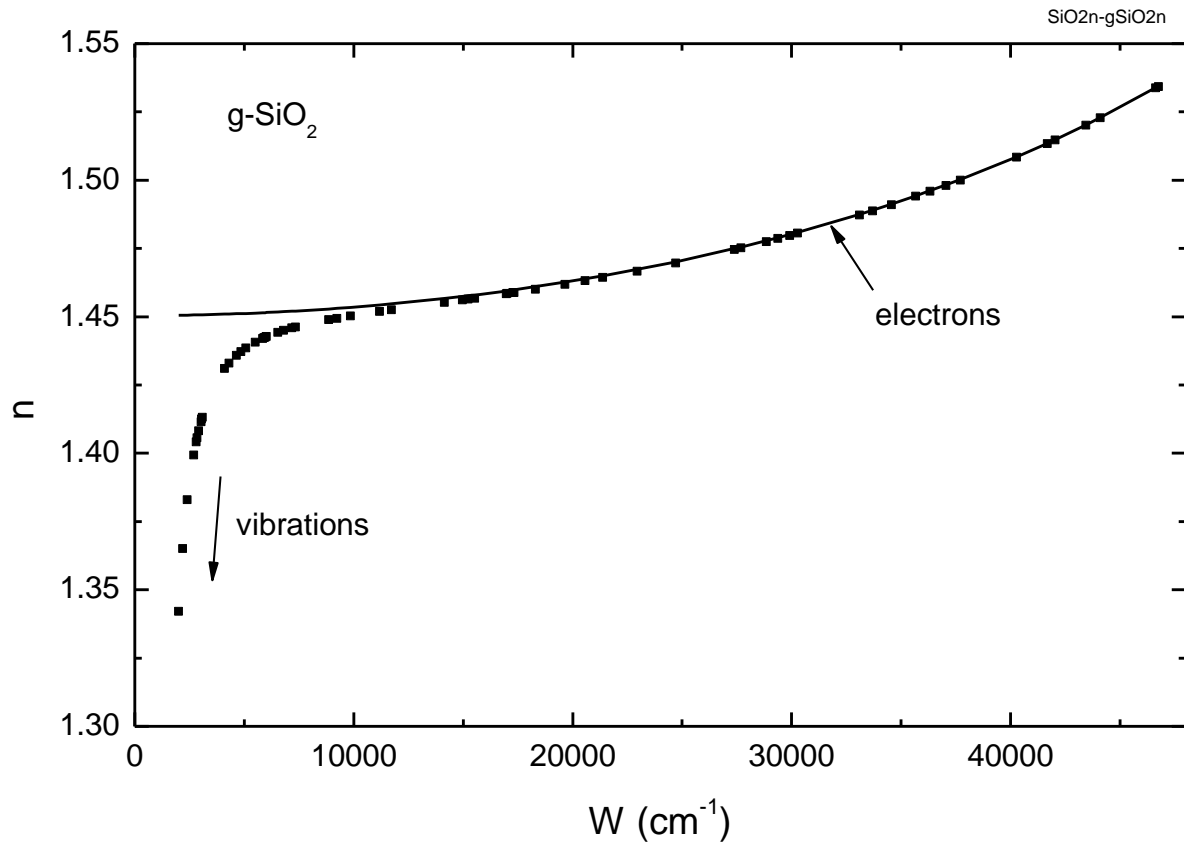
Broad vibrational bands (nearly Gaussian profiles) in three ranges of phononic structures of crystalline SiO₂



Transparent range between vibrational (IR) and electronic (UV) absorption: g-SiO₂

Even powers expansions of the refractive index or dielectric function identify the vibronic and electronic contribution to the dispersion.

Data points: several minimum-deviation measurements on prisms (from Palik's handbook); attaining the high level of precision requires stringent control of temperature and other conditions.



Optical glasses

utilize the transparent range between vibrational and electronic absorption

refractive index at selected wavelengths
from visible range
and
dispersive power / Abbe number

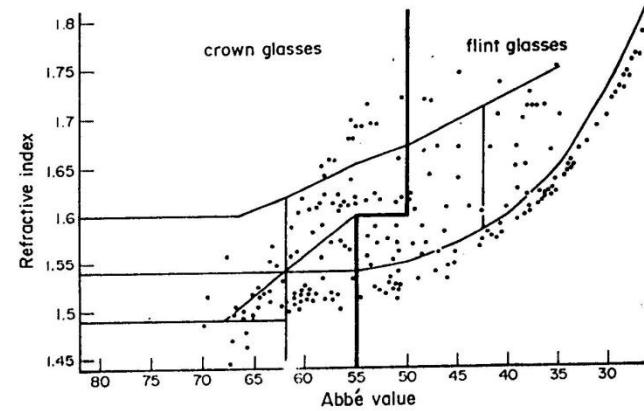


Figure 1
Refractive index against Abbe value diagram

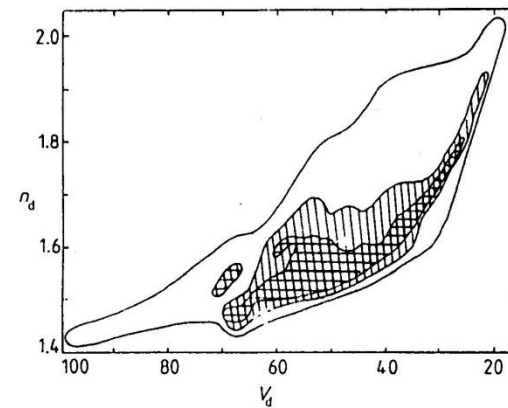


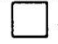


Figure 3.2 Reciprocal dispersive power $(n_d - 1)/(n_f - n_c)$ plotted against n_d for commercial optical glasses (Gliemeroth 1982). 1881 , 1939 , 1981 .

Transparent range between vibrational (IR) and electronic (UV) absorption

very small attenuation should be observed in heavy (fluoride) glasses

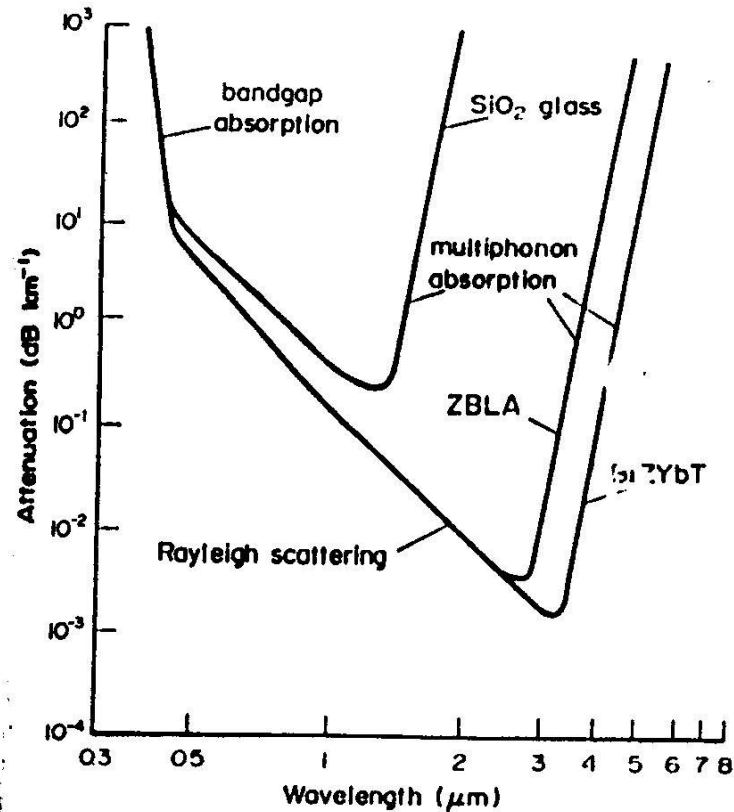


Figure 6
Ultratransparency region (very low absorption) for fluoride and SiO₂ glasses

Recommended reading

A number of textbooks and monographs dealing with the electrodynamics at optical frequencies:

Feynman, Landau-Lifshitz, Born-Wolf, Wooten, Dressel-Gruener, Yu-Cardona, ...

Layered systems interacting with polarized light are dealt with in detail in “Handbook of Ellipsometry” (edited by Irene and Tompkins).

Several topics concerning mainly present-day ellipsometry are dealt with in “Ellipsometry at nanoscale” (edited by Losurdo and Hingerl).

A good deal of discussion of individual materials in the “critiques” of Palik’s Handbooks.